Chemical Engineering Journal 218 (2013) 108–115

Contents lists available at SciVerse ScienceDirect

Chemical Engineering Journal

journal homepage: www.elsevier.com/locate/cej

Enrichment of polychlorinated biphenyl 28 from aqueous solutions using Fe_3O_4 grafted graphene oxide

Shaolin Zeng [a], Ning Gan [a,*], Rebecca Weideman-Mera [b], Yuting Cao [a], Tianhua Li [a], Weiguo Sang [a]

[a] The State Key Laboratory Base of Novel Functional Materials and Preparation Science, Faculty of Material Science and Chemical Engineering, Ningbo University, Ningbo 315211, China
[b] Department of Chemistry, Delaware State University, 1200 N. DuPont Highway, Dover, DE 19901, United States

HIGHLIGHTS

- Using Fe_3O_4@GO as the sorbent of MSPE.
- The first time using Fe_3O_4@GO to adsorb trace levels of PCBs in water samples.
- Investigation of Fe_3O_4@GO's adsorption characteristics and sorption isotherm.
- Establishment of a highly selective and sensitive MSPE–GC–MS analytical method.

ARTICLE INFO

Article history:
Received 10 October 2012
Received in revised form 7 December 2012
Accepted 8 December 2012
Available online 17 December 2012

Keywords:
Fe_3O_4 nanoparticles
Graphene oxide
Magnetic solid-phase extraction
PCB 28
Trace levels

ABSTRACT

In this paper, Fe_3O_4 nanoparticle (Fe_3O_4 NPs) grafted graphene oxide (Fe_3O_4@GO), are successfully synthesized and used for the extraction of 2,4,4′-trichlorobiphenyl (PCB 28) from a large volume of water solution. With the magnetic solid-phase extraction (MSPE) technique based on the Fe_3O_4@GO sorbents, it requires only 30 min to extract trace levels of PCB 28 from 200 mL water samples. The Fe_3O_4@GO was analyzed by using powder X-ray diffraction (XRD), transmission electron microscopy (TEM), Fourier Transform infrared (FT-IR) spectroscopy, and Vibrating sample magnetometer (VSM), specific surface area analyzer. The adsorption kinetics, adsorption capacity of the adsorbent, and the effect of the solution pH and desorption conditions on the removal efficiency of PCB 28 were investigated. The second-order kinetic equation best describes the sorption kinetics. The results showed that Fe_3O_4@GO was a suitable material in the pre-concentration and immobilization of PCB 28 from large volumes of aqueous solutions in polychlorinated biphenyl pollution cleaning.

1. Introduction

Polychlorinated biphenyls (PCBs) are a class of chlorinated aromatic hydrocarbon chemicals that are now known as a part of the persistent organic pollutants (POPs) [1]. The occurrence of polychlorinated biphenyls (PCBs) in water systems is currently a major problem of global concern because of their harmful impact on ecosystem health and on the safety of human food supplies [2]. Moreover, PCBs are an example of the typical persistent organic toxins present in the natural environment ubiquitously, and they are highly toxic, resistant to degradation, and have the property of high bioaccumulation [3]. Therefore, the determination of trace PCBs in water samples turned out to be a great challenge due to the poor aqueous solubility of PCBs. The effective enrichment and identification of lowly concentrated PCBs in the environment is attracting a great deal of research attention due to human health concerns [4–9]. Low chlorinated PCBs are significant for the evaluation of the transport and overall fate of PCBs because of their relatively high aqueous solubility [10]. Herein, 2,4,4′-trichlorobiphenyl (PCB 28), a primary congener of toxic PCBs in the environment, is selected as the model substance to investigate the sorption properties of PCBs.

In recent years, a new procedure for SPE, based on the use of magnetic or magnetically modified adsorbents called magnetic solid-phase extraction (MSPE), has been developed [11]. The magnetic adsorbents have emerged as a new generation of materials for environmental decontamination since magnetic separation simply involves applying an external magnetic field to extract the adsorbents. So the separation process in MSPE can be performed directly in crude samples containing suspended solid material without the need of additional centrifugation or filtration, which makes separation easier and faster [12,13]. At the same time, loading of the magnetic nanoparticles can avoid or decrease the possibility of serious agglomeration and restacking of the graphene sheets.

* Corresponding author. Tel./fax: +86 574 87609933.
E-mail addresses: zengshaolin7320@126.com (S. Zeng), ganning@nbu.edu.cn (N. Gan).

1385-8947/$ - see front matter © 2012 Elsevier B.V. All rights reserved.
http://dx.doi.org/10.1016/j.cej.2012.12.030

Now, carbon nanostructure materials, due to their extremely large surface area and excellent adsorption capacity, have been successfully used as the adsorbent in SPE for the trapping or separating of some organic compounds [14,15]. Graphene oxide reduction (rGO) nanoparticles are relatively new adsorbents which have been proven to possess excellent adsorption capacity for aromatic hydrocarbon compounds due to their π–π interactions [16,17]. However, to our knowledge, there is less study concerning the adsorption capacity of persistent organic pollutants in solution with graphene oxide (GO). Chemically derived graphene oxide (GO) from graphite has revealed a variety of potential uses because of its flexibility and relatively cheap fabrication. GO also is an interesting material because of its excellent dispersibility in water, unlike graphite. Therefore, the introduction of magnetic properties into GO would combine the high adsorption capacity of GO and the separation convenience of magnetic materials. This provides a higher available surface area and, therefore, an enhancement of adsorption capacity, owing to the spacing effect of the magnetite nanoparticles between the neighboring graphene oxide sheets.

Recently a few researchers have managed to fabricate magnetic graphene and graphene oxide nanocomposites [18–21]. The magnetic graphene oxide (GO) are relatively new adsorbents and they have been proven to possess excellent adsorption capacity to eliminate many kinds of organic pollutants and heavy metal ions [22–26] from large volumes of wastewaters. The results suggested that Fe_3O_4@GO is very suitable material in the removal of organic and inorganic pollutants from large volumes of aqueous solutions. However, to our knowledge, there has been no report yet about the use of graphene oxide magnetic nanocomposite for the removal of trace levels of POPs from water samples. In the present study, we reported the preparation of Fe_3O_4@GO and their potential applications in the enrichment of PCB 28 from environmental water samples. We had selected six kinds of major toxic PCBs (PCB 28, PCB 52, PCB 101, PCB 138, PCB 153, PCB 180) to evaluate the performance of the method. The nanocomposite was characterized by transmission electron microscopy (TEM), powder X-ray diffraction (XRD), Fourier transform infrared (FTIR) and Vibrating sample magnetometer (VSM), specific surface area analyzer. The adsorption characteristics of this magnetic nanocomposite and the impact of some experimental factors on its adsorption power were also investigated. Coupling this novel MSPE technique with GC–MS separation and detection, a highly selective and sensitive MSPE–GC–MS analytical method was established.

2. Experimental

2.1. Chemicals and materials

PCB 28 was obtained from Accu Standard (New Haven, CT, USA). Graphite powder (purity 99.9995%) and sulfuric acid (95–97%) were obtained from Aladdin Chemistry Co. Ltd. Ferric chloride hexahydrate ($FeCl_3{\cdot}6H_2O$), ferrous chloride tetrahydrate ($FeCl_2{\cdot}4H_2O$), sodium hydroxide, ammonia, n-hexane and dichloromethane were purchased from Beijing Chemicals Corporation (Beijing, China). The syringe filters was purchased from Xingya (Shanghai). All reagents used in the experiment were of analytical reagent grade and used without further purification.

2.2. Preparation of GO

The graphite oxide was synthesized from natural graphite powder based on a modified Hummers method [27–29]. Then, exfoliation of graphite oxide to GO was achieved by ultrasonication for 1 h (200 W, 40 kHz). Finally, a homogeneous GO aqueous dispersion was obtained and used for further characterization.

2.3. Synthesis of Fe_3O_4@GO

The magnetic graphene oxide-Fe_3O_4 nanoparticles hybrid (Fe_3O_4@GO) was synthesized by the in situ chemical co-precipitation of Fe^{2+} and Fe^{3+} in an alkaline solution in the presence of GO. Firstly, 100 mL GO (3 mg mL^{-1}) aqueous was sonicated for 1 h to transform the carboxylic acid groups to carboxylate anions. Then the solution of 0.02 mol of $FeCl_3{\cdot}6H_2O$ and 0.01 mol of $FeCl_2{\cdot}4H_2O$ in water (10 mL) was purged with N_2 for 30 min. This solution was added dropwise to the GO solution at room temperature under a nitrogen flow (30 mL min^{-1}) with vigorous stirring for 2 h. Then a 28% ammonia solution was added drop by drop (with dropping rate of 10 d min^{-1}) to give the solution pH 11–12 for synthesis of magnetic Fe_3O_4 NP. The mixture was kept stirring at 65 °C for a further 2 h. Then the mixture was washed thoroughly with water to neutral pH and dried under vacuum at 40 °C [30,31].

2.4. Material characterization

The particle size and structure of the sorbents were observed by using a JEOL 2100 transmission electron microscope (TEM). The infrared (IR) spectra of the obtained sorbents were taken in KBr pressed pellets on a NEXUS 670 infrared Fourier transform spectrometer (Nicolet Thermo, Waltham, MA). Magnetic property was analyzed using a vibrating sample magnetometer (VSM, LDJ9600). The XRD characterization was performed using X-ray diffraction (Bruker, D8 Focus) with Cu Kα radiation at room temperature. The surface areas were determined by nitrogen adsorption–desorption isotherms (ASAP 2020, Micromeritics Co., USA).

2.5. Adsorption experiments

The removal of PCB 28 from aqueous solutions by the Fe_3O_4@GO sorbents was carried out using following experimental procedures. The standard stock solution (14.7 mg L^{-1}) of PCB 28 was prepared in n-hexane and stored at 0 °C. All the working solutions of PCB 28 were 1.47 mg L^{-1} and prepared daily by appropriate dilution of the stock solutions with ultra-pure water. The adsorption experiments were carried out in beakers at room temperature. Firstly, 0.05 g of the Fe_3O_4@GO sorbents were rinsed and activated in 2 mL of methanol, and then dispersed into 200 mL working solutions. The mixture was sonicated for 5 min and stirred for 60 min. Subsequently, an Nd–Fe–B strong magnet was deposited at the bottom of the beaker and the sorbents were isolated from the solution. After about 30 s, the solution became clear and the supernatant was decanted. The adsorption process is shown in Fig. 1.

2.6. Desorption studies

For the desorption step, firstly, the pre-concentrated analytes were transferred to the syringes of organic membrane (0.45 μm), drying at 40 °C under vacuum for 1 h. Secondly, 14 mL n-hexane/dichloromethane (70:30, v/v) mixture was injected into the syringe with infusion pump at 2 mL min^{-1} and the eluate was collected with the 15 mL centrifugal tubs. Thirdly, the eluate was dried with a stream of nitrogen at 40 °C and the residue was dissolved in 1 mL of n-hexane with concentrated sulfuric acid to further acidification. Finally, 1 μL of the supernate was injected rapidly into the gas chromatograph for the analysis by GC–MS.

2.7. GC–MS analysis

The GC–MS analysis was performed on SHIMADZU QP2010E GC–MS system equipped with a DB-5 MS column (30 m × 0.25 mm I.D. × 0.25 μm film thickness). The temperatures of injector and ion source were 280 °C and 220 °C, respectively. A 1 μL sample was

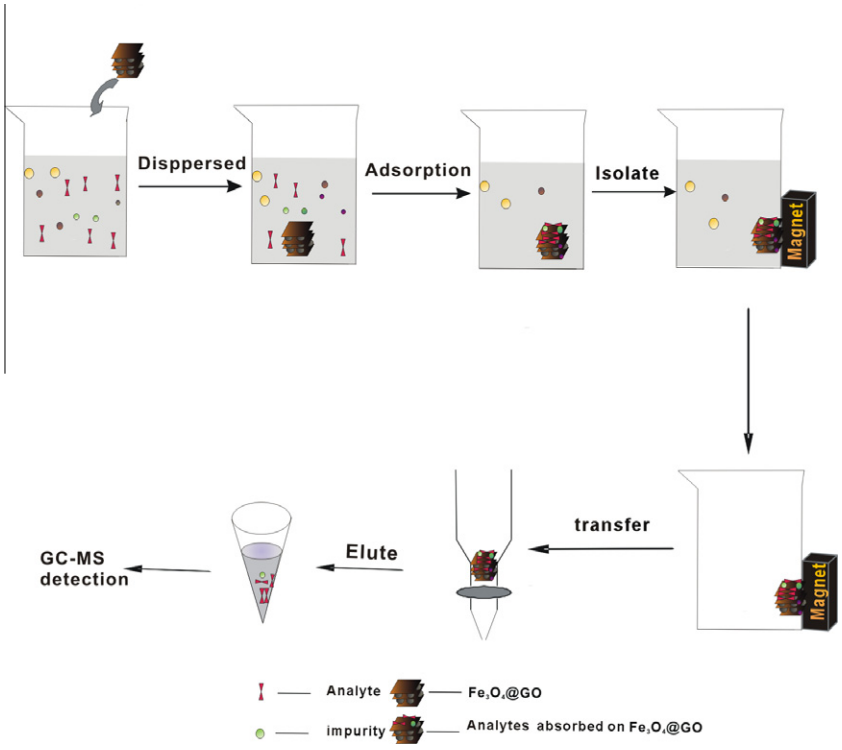

Fig. 1. Adsorption process.

injected manually in split stream mode. The carrier gas was helium at 0.7 mL min^{-1}. The oven temperature was programmed as follows: initial temperature 110 °C for 3 min, heated to 230 °C at 20 °C $min^{-1}$and held for 5 min, then ramped at 5 °C min^{-1} to 250 °C and held for 2 min, finally ramped at 20 °C min^{-1} to 290 °C; EI (70 eV); ion source temperature 220 °C; scan range 45–650 amu s^{-1}; solvent delay time 7 min. Selected ion monitoring (SIM) was used to quantify the analytes.

3. Results and discussion

3.1. Characterization of sorbents

The XRD pattern of the GO, Fe_3O_4 and Fe_3O_4@GO are presented in Fig. 2a. The appearance of diffraction peak at $2\theta = 10.3°$ (001) could be ascribed to the reflection of the GO. Six diffraction lines are observed in the representative XRD pattern of Fe_3O_4 at $2\theta = 30.1°$, 35.4°, 43.3°, 54.5°,57.3° and 62.8°. These diffraction lines can be assigned to the (220), (311), (400), (422), (511) and (440) reflections, respectively, of the pure cubic spinel crystal structure of Fe_3O_4 with cell constant $\alpha = 8.397$ Å (JCPDS card no. 19-0629). From the XRD pattern of Fe_3O_4@GO analysis, the main characteristic peaks of Fe_3O_4 and GO are located at 10.3°, 30.1°, 35.4°, 43.3°, 54.5°, 57.3°and 62.8°, indicating that the product is composed of two phases: Fe_3O_4 and GO.

The magnetic property of the Fe_3O_4@GO nanocomposite is investigated by VSM. Fig. 2b shows the supermagnetization curves of Fe_3O_4 (0.005 g) and Fe_3O_4@GO (0.0049 g) at room temperature. Maximum saturation supermagnetizations of Fe_3O_4 and Fe_3O_4@GO are measured at 51.57 and 43.85 emu g^{-1}, respectively. Although the addition of nonmagnetic portion leads to decreased saturation supermagnetizations, the obtained Fe_3O_4@GO still have a high saturation supermagnetization of 43.85 emu g^{-1}. According to Ma's study, a saturation supermagnetization of 16.3 emu g^{-1} is enough for magnetic separation from solution with a magnet [32]. These imply that Fe_3O_4@GO sorbents can be dispersed into water solution readily and the magnetic sorbent loaded with analytes can be isolated from the matrix conveniently by using an external magnet when necessary. Once the external magnetic field is taken away, these sorbents can re-disperse rapidly.

The microstructure transformations and differences of GO, Fe_3O_4 and Fe_3O_4@GO can be observed by TEM images (Fig. 3). As to exfoliated GO (Fig. 3A), large sheets (a few 100 square nanometers) were observed to be situated on the top of the grid, where they resembled silk veil waves. They were transparent and entangled with each other. On the basis of the HR-TEM image (Fig. 3B), the planar space of lattice fringes is about 0.5 nm. And the selected area electron diffraction (SAED) pattern indicates that GO nanoparticles are polycrystals. Fig. 3C shows the TEM images of (Fe_3O_4 NPs). Fe_3O_4 NPs appear quasi-spherical in shape with an average diameter of about 20 nm. Fig. 3D shows that the Fe_3O_4 particles uniformly disperse on graphene oxide sheets. We can see that the small Fe_3O_4 particles are also polycrystals. And the BET surface area of Fe_3O_4@GO is 145.8 m^2 g^{-1}.

Fig. 4 shows the FTIR spectra of GO and Fe_3O_4@GO powders. The intense bands at 3450 and 1250 cm^{-1} are attributed to stretching of the O—H band of CO—H. The band at 1680 cm^{-1} is associated with stretching of the C=O bond of carboxyl groups. Deformation of the C—O band is observed at the band present at 1100 cm^{-1}. The FTIR spectrum of Fe_3O_4@GO differs from that of GO as evidenced by the weakening of the peak at 3450 cm^{-1}. Moreover, the peak at 580 cm^{-1} can be ascribed to lattice absorption of iron oxide, indicating the strong interaction of the nanoparticles with O [33].

3.2. Kinetics analysis

The effect of adsorption time on the removal of PCB 28 by the Fe_3O_4@GO nanocomposite is shown in Fig. 5. The result indicates that a fast adsorption process of the PCB 28 occurred during the first few minutes and the adsorbed amount of the PCB 28 reached its equilibrium value very quickly. It was observed that the equilibrium time for PCB 28 was about 30 min.

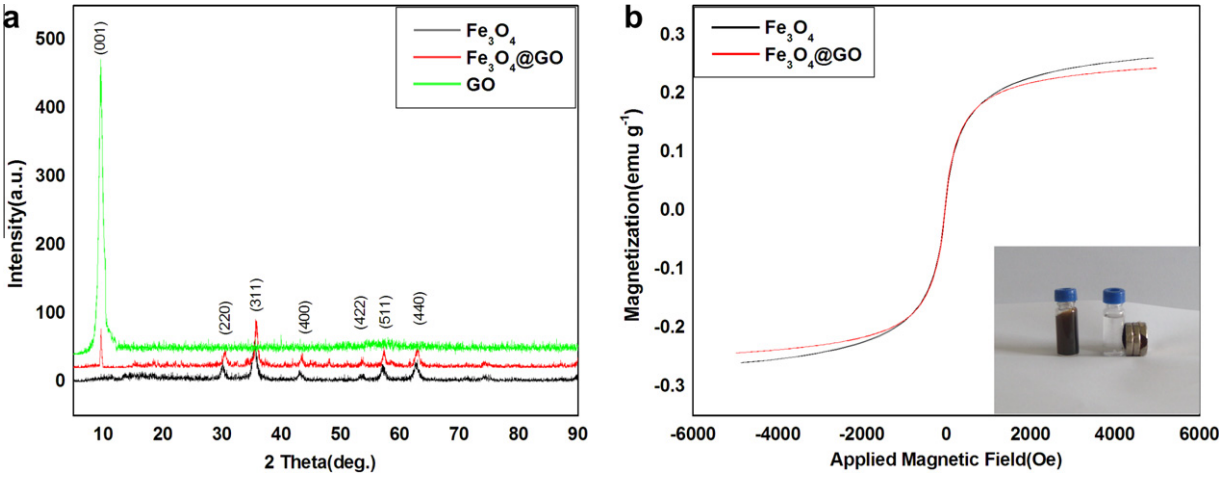

Fig. 2. (a) X-ray diffraction (XRD) patterns of GO, Fe_3O_4 and Fe_3O_4@GO; (b) vibrating sample magnetometer (VSM) supermagnetization curves of Fe_3O_4 and Fe_3O_4@GO, the inset picture in (b) shows the Fe_3O_4@GO dispersed in the PCB 28 solution and magnetic separation.

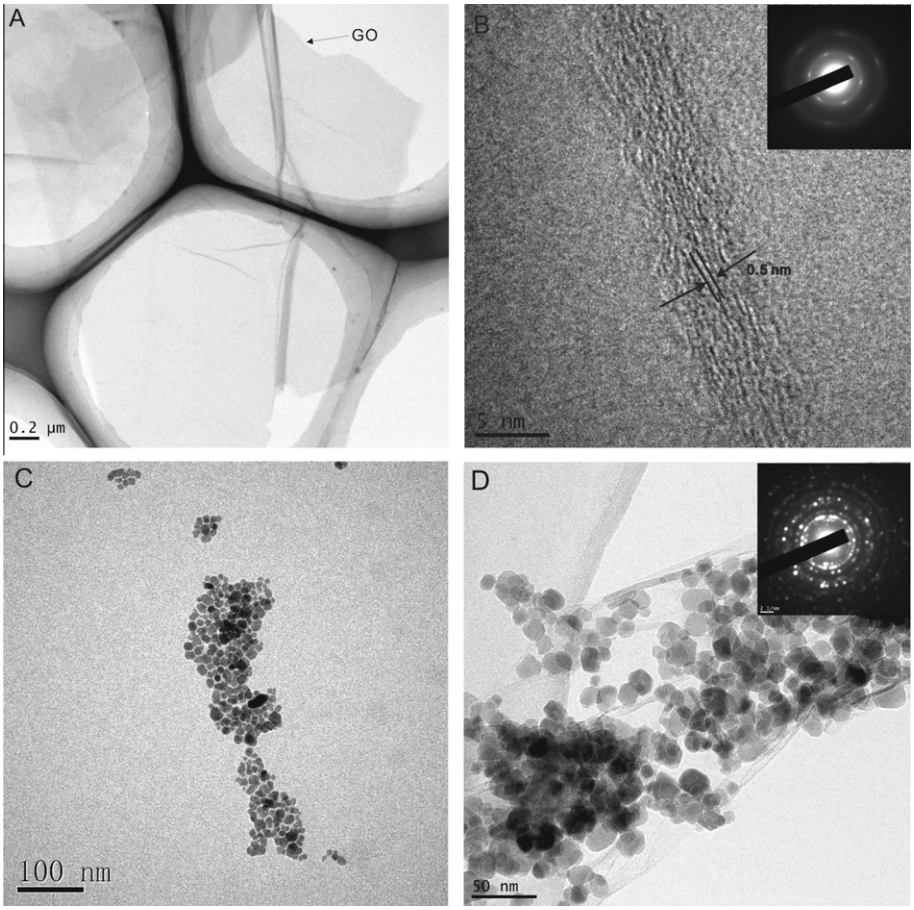

Fig. 3. Transmission electron microscope (TEM) images of (A) graphene oxide (GO), (C) Fe_3O_4 and (D) Fe_3O_4@GO; (B) HR-TEM image of the nanoparticles of the composite with the inset image, the inset in (B and D) depict the corresponding SAED pattern of GO and Fe_3O_4@GO.

In order to show the most suitable model for the experimental data, two different kinetic models were used in this study. They are pseudo-first-order rate model and pseudo second-order rate model. Pseudo-first-order rate equation is expressed as follows:

$$\ln(q_e - q_t) = \ln q_e - kt \quad (1)$$

where q_e is the amount of PCB 28 (mg g^{-1}) adsorbed per unit mass of adsorbent at equilibrium, q_t is the amount of PCB 28 (mg g^{-1}) adsorbed at time t (min^{-1}), and k is the equilibrium rate constant of pseudo first-order. The pseudo second-order model can be expressed as follows:

$$\frac{t}{q_t} = \frac{1}{k_1 q_e^2} + \frac{1}{q_e} t \quad (2)$$

where k_1 (g mg^{-1} min^{-1}) is the pseudo second-order rate constant. Based on the two models, curve fitting was performed and the

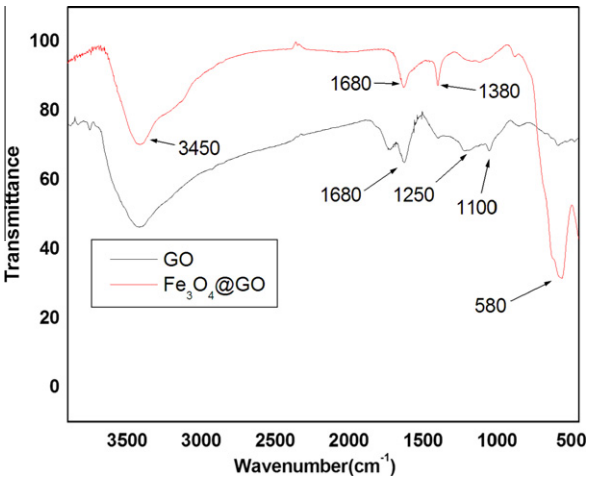

Fig. 4. IR spectra of (a) GO and (b) Fe_3O_4@GO.

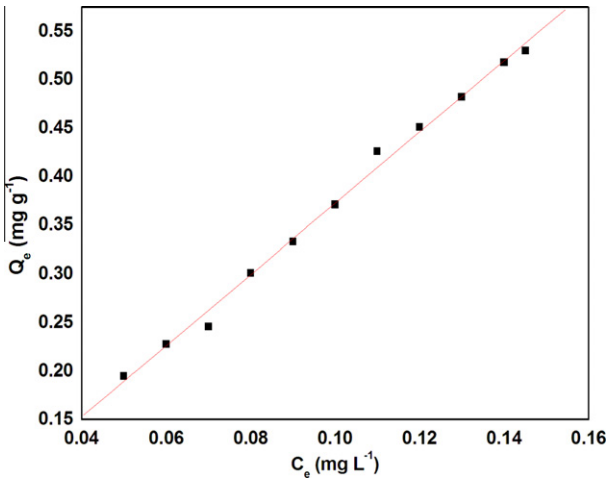

Fig. 6. Sorption isotherm of PCB 28 on Fe_3O_4@GO.

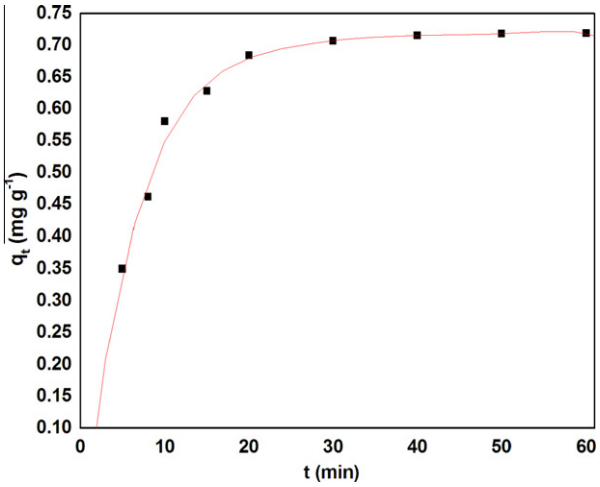

Fig. 5. Effect of adsorption time on the adsorbed amount of PCB 28 by Fe_3O_4@GO nanocomposites.

parameters in the models and regression coefficients (R^2) for the two kinetic models were obtained. For PCB 28, R^2 for the pseudo-first-order and pseudo second-order equations were 0.986 and 0.9972, respectively. For the pseudo-first-order model, the calculated values of q_e and k were 0.725 mg g^{-1} and 0.135 min^{-1}, respectively. The experimental q_e value of 0.708 mg g^{-1} was consistent with the q_e value calculated from the pseudo-first-order model. For the pseudo-second-order model, the experimental values of q_e and k_1 were 0.718 mg g^{-1} and 0.262 g mg^{-1} min^{-1}, respectively. It was indicated that experimental kinetic data for PCB 28 adsorption by Fe_3O_4@GO followed the pseudo-second-order rate model better than the pseudo-first-order model.

3.3. Adsorption isotherms

Sorption isotherm is important to understand the sorption properties of PCB 28 on Fe_3O_4@GO. The experiment used 50 mg Fe_3O_4@GO to absorb saturated concentration (0.147 mg L^{-1}) [34] of PCB 28 in 200 ml water solution. We found that Fe_3O_4@GO's absorption mechanism to PCB is still linear in Fig. 6 which suggests that the sorption of PCB 28 is far from saturation. The large sorption ability of PCB 28 on Fe_3O_4@GO indicates that Fe_3O_4@GO is a very suitable material in the removal of PCB 28 from large volumes of aqueous solutions. Yang et al. [35] reported that 2,4,5-trichlorobiphenyl (2,4,5-TCB) was rapidly adsorbed on activated carbon felt (ACF) and the sorption of 2,4,5-TCB on ACF was irreversible chemical sorption. Pan and Xing [36] reported that benzene rings may act as hydrogen bond donors and form hydrogen bonds with oxygen-containing functional groups on organic chemicals. Therefore, PCB 28 can form hydrogen bonds and electron donor–acceptor interactions with the introduced functional groups of GO on Fe_3O_4@GO surfaces.

3.4. Optimization of extraction conditions

In this experiment, several parameters, including sample pH and desorption conditions were investigated to achieve the best extraction efficiency for the PCB 28. 200 mL double-distilled water spiked with 100 ng mL^{-1} of PCB 28 was used for the study of the extraction performance of the MSPE under different experimental conditions. All the experiments were performed in triplicate and the means of the results were used for optimization.

3.4.1. Effect of the solution pH

Solution pH can play an important role for the adsorption of the analytes by affecting both the existing forms of the target compounds and the charge species and density on the sorbent surface. In this work, the effect of solution pH on the extraction of target is investigated in the pH range of 3.0–10.0. As can be seen from Fig. 7a, the sorption percentage of PCB 28 on Fe_3O_4@GO fluctuates very little in pH range of 3–8, which suggests that Fe_3O_4@GO are excellent adsorbents for PCBs' removal from large volumes of aqueous solutions. When the pH is greater than 8, the sorption percentage of PCB 28 on Fe_3O_4@GO decreases with increasing pH values. This can be ascribed to the fact that more oxygen containing groups (such as —COOH and —OH) on Fe_3O_4@GO surfaces are ionized (carrying negative charge) at high pH values. More water molecules are then adsorbed to prevent PCB 28 from getting closed to the adsorbent. The formation of a water cluster on oxygen-containing groups blocks the access of PCB 28 to the adsorption sites of Fe_3O_4@GO and thereby results in less adsorption of PCB 28. As seen from our experiment, the pH independent adsorption of PCB 28 on Fe_3O_4@GO at pHs less than 8 is quite important for the application of Fe_3O_4@GO in PCB 28 pollution cleanup in real work.

3.4.2. Desorption conditions

The most commonly used solvents are dichloromethane and n-hexane in PCB 28 analysis. In this study, we also apply these solvents to elute PCB 28 from the Fe_3O_4@GO-SPE syringe. Moreover,

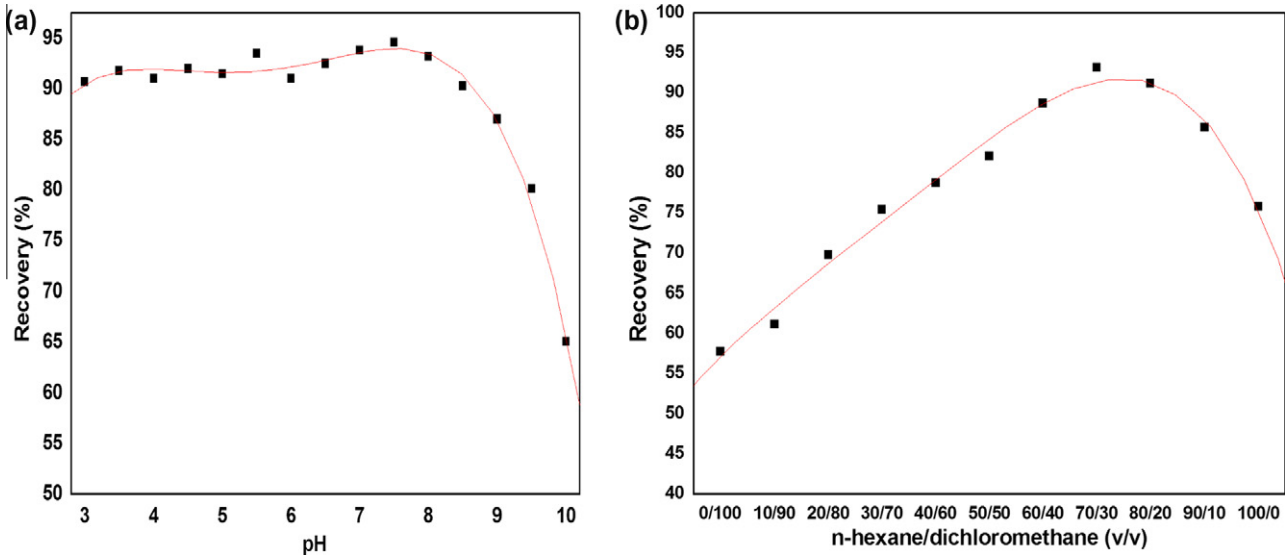

Fig. 7. (a) Effects of pH values on the recoveries of PCB 28; (b) effects of solvent type on the recoveries of PCB 28.

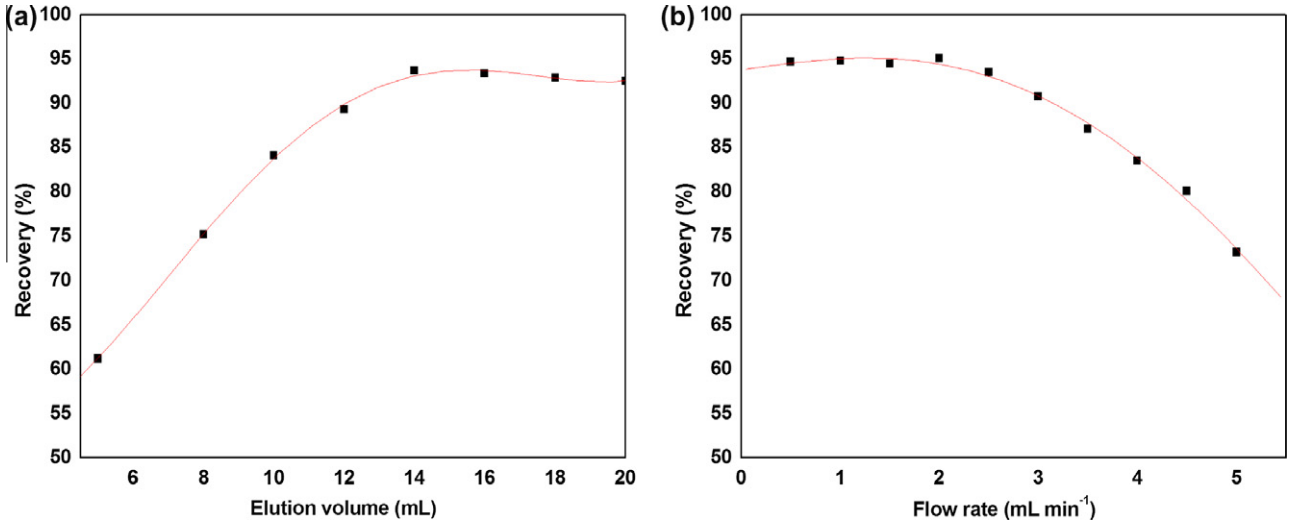

Fig. 8. (a) Effects of volume on the recoveries of PCB 28; (b) effects of elution flow rate on the recoveries of PCB 28.

Table 1
Comparison of Fe_3O_4@GO-SPE with other extraction methods for the determination of PCB 28 in water samples.

Methods	LODs (ng mL^{-1})	RR (%)	Time of pretreatment (h)
GO-SPE	0.028–0.051	70.9–97.5	6.4
Fe_3O_4@GO-SPE	0.027–0.059	77.2–99.7	3.0
C18–NH_2–SPE	0.007–0.023	74.6–101.4	6.0

the recoveries of PCB 28 were compared by the proportion of mixture which was loaded at 2.5 mL on the syringe. As the results shown in Fig. 7b, different solvents possess different elution efficiency. N-hexane is known as a non-polar solvent and dichloromethane is a polar solvent with a polarity index of 3.1. In fact, the mixture of n-hexane and dichloromethane is often used to elute PCBs from silica gel column due to its proper polarity index. The performance of n-hexane/dichloromethane (70:30) is better and more stable than other proportions of the mixture. Therefore, the mixture of n-hexane/dichloromethane (70:30) becomes the solvent to elute the Fe_3O_4@GO-SPE syringe in the following tests.

To study the effect of desorption volume, desorption solvent amounts from 4 mL to 20 mL are used to elute the analytes after sample extraction and the washing step. From the Fig. 8a, the target is eluted by 14 mL of n-hexane/dichloromethane (70:30), and the recoveries of PCB 28 exceeded 91% at 14 mL. After elution, volume becomes higher than 14 mL, recovery rates do not increase; they even occasionally decrease. In addition, less than 14 mL of n-hexane/dichloromethane (70:30, v/v) mixture cannot elute the extracted PCB 28 from the Fe_3O_4@GO-SPE syringe totally. Therefore, 14 mL of n-hexane/dichloromethane (70:30) become the best choice to elute PCB 28 from the Fe_3O_4@GO-SPE syringe in the following tests.

The desorption flow rate is optimized in the range of 0.5–5 mL min^{-1}. Low flow rate may prolong the whole analysis time while too high of a flow rate may cause high back pressure which will not favor the operation of extraction. In the Fig. 8b, although the recovery rate of the desorption flow rate of 0.5–1.5 mL are relatively high, the elution time becomes quite long. When the flow rates go over 2 mL min^{-1}, the recovery rates of the PCB 28 begin to decline. This is probably because that the speed of flow rate is

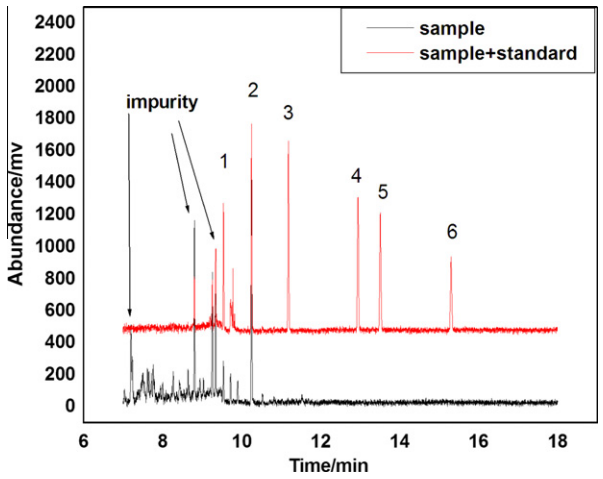

Fig. 9. Chromatographs of school water and school water samples spiked with 10 ng mL^{-1} of PCBs. The samples were analyzed via GC–MS. Peak identification: (1) PCB 28, (2) PCB 52, (3) PCB 101, (4) PCB 153, (5) PCB 138, (6) PCB 180.

too fast, while the PCB 28 is still partly retained on the absorbent, causing the recovery rate to decline. Therefore, a flow rate of 2 mL min^{-1} is chosen to obtain satisfactory desorption efficiency within a short time.

3.5. Comparison of Fe_3O_4@GO-SPE with other extraction methods of PCB 28

We have investigated the Fe_3O_4 and the reduced GO/Fe_3O_4 composites on the adsorption of PCB 28. We found that there was no signal when we used the Fe_3O_4 only. And the reduced graphene and graphene oxide on the adsorption of PCB 28 almost had the similar signal. We guess that is because the concentration of PCB 28 is very low in the solution. So in the same concentration factor cases, Table 1 summarized the LODs, relative recovery (RR) and analysis time and comparison of GO-SPE, Fe_3O_4@GO-SPE and C18–NH_2–SPE, the extraction and determination of PCB 28 in water samples, expressed as mean value ($n = 3$). In the experiment, we employ all the materials except Fe_3O_4@GO-SPE as stationary phase of SPE to enrich and purify PCB 28 in aqueous solutions. The recoveries of PCB 28 range from 70.9% to 97.5%, 77.2% to 99.7% and 74.6% to 101.4% for GO-SPE, Fe_3O_4@GO-SPE and C18–NH_2–SPE methods, respectively. From Table 1, we can see that the method of Fe_3O_4@GO-SPE is the most time-saving with its simple operation, which only took 3.0 h. The results also show Fe_3O_4@GO-SPE is an efficient and simple method to analyze PCB 28 in sewage water samples.

3.6. Determination of PCBs in environmental water samples

To test the Fe_3O_4@GO-SPE method, this paper analyzes school water, and river water samples. We had selected six kinds of major toxic PCBs (PCB 28, PCB 52, PCB 101, PCB 138, PCB 153, PCB 180) to evaluate the performance of the method. As shown in Fig. 9, the results indicated that school water was contaminated by PCB 28 and PCB 52.

4. Conclusions

In this study, magnetic nanoparticles were successfully synthetized, functionalized with GO groups to improve their hydrophilicity and dispersibility in aqueous solution, and had been characterized by TEM, XRD, FTIR and VSM techniques. Through a chemical deposition method, Fe_3O_4 nanoparticles in size of about 10–20 nm were homogeneously dispersed onto graphene oxide sheets. The results presented in this work regarding the kinetics and equilibrium of PCB 28 adsorption, showed that Fe_3O_4@GO had great potential as an effective absorbent for removing PCB 28 in water solution. Kinetic data of PCB 28 adsorption on Fe_3O_4@GO can be satisfactorily described by a pseudo second-order kinetic model. With the magnetic solid-phase extraction (MSPE) technique based on the Fe_3O_4@GO sorbents, it requires only 30 min to extract trace levels of PCB 28 from 200 mL water samples. When the eluate condensed to 1.0 mL, concentration factors for PCB 28 became over 200. To combine SPE technique with gas chromatography–mass spectrometry (GC–MS) detection, a highly efficient and fast SPE–GC/MS analytical method was established.

Acknowledgments

This work was supported by the Natural Science Foundation of Zhejiang Province (LY12C20004, Y3110479), the Natural Science Foundation of Ningbo(2011A610018, 2012A610144), the KC Wong Magna Fund in Ningbo University.

References

[1] P. Liu, D.J. Zhang, J.H. Zhan, Investigation on the inclusions of PCB 52 with cyclodextrins by performing DFT calculations and molecular dynamics simulations, Phys. Chem. A 114 (2010) 13122–13128.
[2] R. Sawicki, L. Mercier, Evaluation of mesoporous cyclodextrin–silica nanocomposites for the removal of pesticides from aqueous media, Environ. Sci. Technol. 40 (2006) 1978–1983.
[3] D.D. Shao, G.D. Sheng, C.L. Chen, X.K. Wang, N. Masaaki, Removal of polychlorinated biphenyls from aqueous solutions using β-cyclodextrin grafted multiwalled carbon nanotubes, Chemosphere 79 (2010) 679–685.
[4] M.T. Li, G.W. Meng, Q. Huang, Z.J. Yin, M.Z. Wu, Z. Zhang, M.G. Kong, Prototype of a porous ZnO SPV-based sensor for PCB detection at room temperature under visible light illumination, Langmuir 26 (2010) 13703–13706.
[5] M.S. Maria, G. Veronica, Detection and quantitative analysis of organochlorine compounds (PCBs and DDTs) in deep sea fish liver from Mediterranean Sea Perrone, Environ. Sci. Pollut. Res. 17 (2010) 968–976.
[6] Q. Zhou, Y. Yang, J. Ni, Z.C. Li, Z.J. Zhang, Rapid detection of 2,3,3′,4,4′-pentachlorinated biphenyls by silver nanorods-enhanced Raman spectroscopy, Phys. E Low – Dimens. Syst. Nanostruct. 42 (2010) 1717–1720.
[7] Y. Wei, L.T. Kong, R. Yang, L. Wang, J.H. Liu, X.J. Huang, Electrochemical impedance determination of polychlorinated biphenyl using a pyrene cyclodextrin-decorated single-walled carbon nanotube hybrid, Chem. Commun. 47 (2011) 5340–5342.
[8] Q.R. Long, R.T. Yang, Carbon nanotubes as superior sorbent for dioxin removal, J. Am. Chem. Soc. 123 (2001) 2058–2059.
[9] D.D. Shao, J. Hua, X.K. Wang, M. Nagatsu, Plasma induced grafting multiwall carbon nanotubes with chitosan for 4,4-dichlorobiphenyl removal from aqueous solution, Chem. Eng. J. 177 (2011) 498–504.
[10] A. Adeel, R.G. Luthy, D.Z. Dzombak, S.B. Roy, J.R. Smith, Leaching of PCB compounds from untreated and biotreated sludge–soil mixtures, Contam. Hydrol. 28 (1997) 289–309.
[11] Š. Mirka, Š. Ivo, Magnetic solid-phase extraction, J. Magn. Magn. Mater. 194 (1999) 108–112.
[12] S. Zdenka, S. Mirka, S. Ivo, Magnetic ovalbumin and egg white aggregates as affinity adsorbents for lectins separation, Biochem. Eng. J. 40 (2008) 542–545.
[13] M.R. Lidia, V.H. Antonio, H.B. Javier, A.R.D. Miguel, Carbon nanotubes: solid-phase extraction, J. Chromatogr. A 1217 (2010) 2618–2641.
[14] K. Yang, B.S. Xing, Adsorption of organic compounds by carbon nanomaterials in aqueous phase: Polanyi theory and its application, Chem. Rev. 110 (2010) 5989–6008.
[15] M.J. Allen, V.C. Tung, R.B. Kaner, Honeycomb carbon: a review of graphene, Chem. Rev. 110 (2010) 132–145.
[16] H.M. Sun, L.Y. Cao, L.H. Lu, Magnetite/reduced graphene oxide nanocomposites: one step solvothermal synthesis and use as a novel platform for removal of dye pollutants, Nano. Res. 4 (2011) 550–562.
[17] N.W. Li, M.B. Zheng, X.F. Chang, G.B. Ji, H.L. Lu, L.P. Xue, L.J. Pan, J.M. Cao, Preparation of magnetic $CoFe_2O_4$-functionalized grapheme sheets via a facile hydrothermal method and their adsorption properties, J. Solid State Chem. 184 (2011) 953–958.
[18] J.F. Shen, Y.Z. Hu, M. Shi, N. Li, H.W. Ma, M.X. Ye, One step synthesis of graphene oxide-magnetic nanoparticle composite, Phys. Chem. C 114 (2010) 1498–1503.
[19] H.P. Cong, J.J. He, Y. Lu, S.H. Yu, Water-soluble magnetic-functionalized reduced graphene oxide sheets: in situ synthesis and magnetic resonance imaging applications, Small 6 (2010) 169–173.
[20] V. Chandra, J. Park, Y. Chun, J.W. Lee, I.C. Hwang, K.S. Kim, Water-dispersible magnetite-reduced graphene oxide composites for arsenic removal, ACS Nano 4 (2010) 3979–3986.

[21] F. He, J.T. Fan, D. Ma, L.M. Zhang, C. Leung, H.L. Chan, The attachment of Fe3O4 nanoparticles to graphene oxide by covalent bonding, Carbon 48 (2010) 3139–3144.
[22] G.D. Sheng, Y.M. Li, X. Yang, X.M. Ren, S.T. Yang, J. Hu, X.K. Wang, Efficient removal of arsenate by versatile magnetic graphene oxide composites, RSC Adv. 2 (2012) 12400–12407.
[23] X. Yang, C.L. Chen, J.X. Li, G.X. Zhao, X.M. Ren, X.K. Wang, Graphene oxide–iron oxide and reduced graphene oxide–iron oxide hybrid materials for the removal of organic and inorganic pollutants, RSC Adv. 2 (2012) 8821–8826.
[24] J. Li, S.W. Zhang, C.L. Chen, G.X. Zhao, X. Yang, J.X. Li, X.K. Wang, Removal of Cu(II) and fulvic acid by graphene oxide nanosheets decorated with Fe_3O_4 nanoparticles, ACS Appl. Mater. Interfaces 4 (2012) 4991–5000.
[25] M.C. Liu, C.L. Chen, J. Hu, X.L. Wu, X.K. Wang, Synthesis of magnetite/graphene oxide composite and application for Cobalt(II) removal, J. Phys. Chem. C 115 (2011) 25234–25240.
[26] G.X. Zhao, L. Jiang, Y.D. He, J.X. Li, H.L. Dong, X.K. Wang, W.P. Xu, Sulfonated graphene for persistent aromatic pollutant management, Adv. Mater. 23 (2011) 3959–3963.
[27] Y.J. Yao, S.D. Miao, S.Z. Liu, L.P. Ma, H.Q. Sun, S.B. Wang, Synthesis, characterization, and adsorption properties of magnetic Fe_3O_4@graphene nanocomposite, Chem. Eng. J. 184 (2012) 326–332.
[28] T. Hartono, S. Wang, Q. Ma, Z. Zhu, Layer structured graphite oxide as a novel adsorbent for humic acid removal from aqueous solution, Colloid Interface Sci. 333 (2009) 114–119.
[29] P. Bradder, S.K. Ling, S. Wang, S. Liu, Dye adsorption on layered graphite oxide, Chem. Eng. Data 56 (2010) 138–141.
[30] X.Y. Yang, X.Y. Zhang, Y.F. Ma, Y. Huang, Y.S. Wang, Y.S. Chen, Superparamagnetic graphene oxide–Fe_3O_4 nanoparticles hybrid for controlled targeted drug carriers, J. Mater. Chem. 19 (2009) 2710–2714.
[31] C. Wang, C. Feng, Y.J. Gao, X.X. Ma, Q.H. Wu, Z. Wang, Preparation of a graphene-based magnetic nanocomposite for the removal of an organic dye from aqueous solution, Chem. Eng. J. 173 (2011) 92–97.
[32] Z.Y. Ma, Y.P. Guan, H.Z. Liu, Synthesis and characterization of micron-sized monodisperse superparamagnetic polymer particles with amino groups, J. Polym. Sci. Pol. Chem. 43 (2005) 3433–3439.
[33] S.F. Chin, K.S. Iyer, C.L. Raston, Fabrication of carbon nano-tubes decorated with ultra fine superparamagnetic nano-particles under continuous flow conditions, Lab Chip 8 (2008) 439–442.
[34] A.T. Fisk, R.J. Norstrom, C.D. Cymbalisty, D.C.G. Muir, Dietary accumulation and depuration of hydrophobic organochlorines: bioaccumulation parameters and their relationship with the octanol/water partition coefficient, Environ. Toxicol. Chem. 17 (1998) 951–961.
[35] B. Yang, G. Yu, J. Huang, Electrocatalytic hydrodechlorination of 2,4,5-trichlorobiphenyl on a palladium-modified nickel foam cathode, Environ. Sci. Technol. 41 (2007) 7503–7508.
[36] B. Pan, B.S. Xing, Adsorption mechanisms of organic chemicals on carbon nanotubes, Environ. Sci. Technol. 42 (2008) 9005–9013.